Destructive Effects of Plasmas Generated by Exploding Wires

ROBERT C. GOOD JR.*
General Electric Company, Philadelphia, Pa.

A nominal 10-kj capacitor bank is discharged through a 2-mil tungsten wire in an evacuated chamber. The wire material is heated to about 10^{4}°K in the first microsecond. A plasma forms with an ion pair density of about 10^{17} ions/cm^3. Nearby glass walls on the chamber are heated to a condition in which microcracks form on the front surface. Electromagnetic waves from the plasma were focused by an ellipsoidal mirror on a glass surface, and craze-cracks were observed. Photomicrographs of the surfaces show that the number of cracks increases as the energy stored in the capacitors is increased from 400 to 3000 joules. Four main processes are postulated for energy transfer to the glass surface: 1) the hot plasma radiates electromagnetic waves; 2) shock waves form, the strength and propagation characteristics of which depend upon the surrounding media; 3) the hot plasma expands to contact the glass surface; 4) wire particles impact on the surface, creating crater-like pock marks. These processes have been separated, and the effects are reported.

I. Introduction

MANY fundamental mechanisms are involved in the conversion of energy from one form to another; these have been receiving more and more attention in recent investigations. Following this trend, the project discussed herein is concerned with a conversion from electromagnetic to strain energy. A capacitor bank is used to store electrical energy for exploding a 2-mil tungsten wire. The wire heats, melts, vaporizes, and forms a metallic plasma at a temperature of several electron volts. The energy required to heat the metal is several joules,[1, 2] so that the 2000 to 10,000 joules that remain in the capacitor bank are dissipated from the plasma in at least four ways:[3, 4] as black body radiation, as shock waves, as convective heat pulses, and as high-speed wire particles. Of course, these different types of energy transfer are propagated via different paths; therefore, by properly designing the experimental apparatus, the effects of each transfer may be studied separately.

The first, *black body radiation*, covers the whole frequency spectrum, but the waves reaching any point depend upon the absorption of the intermediate media. Thus, the effect may be altered by using different filters. *Shock waves* are formed when a media is present which can support the waves,[5] but only when the mean free path of the particles is less than $\frac{1}{10}$ of the chamber dimensions. Thus, by increasing the mean free path (lowering the pressure of the gas), shock waves may be eliminated. *Convective heat transfer* occurs when the plasma expands to contact or envelop samples within the chamber.[6] The efficiency of this process depends upon the temperature drop with plasma expansion, which is related to the volume expansion before contact. *Particle impact* transfers kinetic energy by mass motion as in convective transfer, but in this case the term refers to the effect of the particles after the plasma disintegrates. Time and distance are the important parameters.

This report describes the experiments conducted to separate the effects of the four methods for transferring energy from the wire to the sample, and it describes the damage caused by each transfer method. In what follows, the equipment is described, the various experiments are discussed, the results are presented, and theoretical arguments are given to explain the results.

II. Experimental Apparatus

An exploding wire facility, built at the Space Sciences Laboratory, is shown in Fig. 1. A high-voltage power supply is used to charge two capacitor banks in series with the explodable wire between them. After charging the capacitors, the high-voltage terminal is shorted to ground, thereby completing the circuit through the wire.[7] Current shunts may be used, or a voltage divider may be connected to the low-voltage side of the wire to trigger the oscilloscopes and record the voltage wave.

Twelve low-inductance type K clamshell inductances can be charged to 80 kv d.c. (40 kv across each bank) in order to store 9600 joules. The ringing frequency is 300 kc, and there are four cycles in each pulse that contain substantial power. In a pulse lasting 10 μsec, the rate of energy dissipation would be about 10^{9} w.

Circuit inductance is minimized by using wide, flat, closely spaced copper plates for the busbars, by using a specially designed feed for the wire, and by using a shorting switch of coaxial design. Two layers of Mylar sheet (0.015 in.) separate the plates and maintain the high electrical field. The shorting switch is a Jennings Manufacturing Company vacuum switch that is mechanically activated by a solenoid with tungsten electrodes forming the spark gap.

The 2-mil tungsten wire is threaded between the apexes of two cones in the central segment of the mirror facility. The center of the wire is placed at the common focus of two intersecting ellipsoids. A close-up view of this cartridge is shown in Fig. 2. The cartridge is open on both ends and includes part of the ellipsoidal mirror located such that the acceptance angle of the individual mirror on either side is almost 180°. The cartridge may be closed without the mirrors by inserting glass windows on either side.

Each of the two symmetrically arranged ellipsoidal mirrors is made in two halves that are bolted together at the plane of the minor axis. Individual halves were shaped from Pyrex tubes collapsed over an ellipsoidal steel mandrel polished to 25-Å surface finish.† The glass was coated with a 400-Å

Presented at the ARS 17th Annual Meeting and Space Flight Exhibition, Los Angeles, Calif., November 13–18, 1962; revision received April 15, 1963. Portions of the work reported here were carried out under a government contract with the Air Force Office of Scientific Research. The contract number was AF 49(638)-1030, Task No. 37718, Project No. 9782; the contract ran from March 1961 through February 1963. The author wishes to thank J. Heyda and A. Garofalo for their assistance with the solutions of the equations, and T. D. Riney and F. W. Wendt for their enlightening discussions of the theory and test results. C. J. Dudzinski prepared the samples and operated the equipment during the tests.

* Space Structures Operation, Space Sciences Laboratory, Space Technology Center.

† Mirrors were made by Fischer and Porter Co., Warminster, Pa.

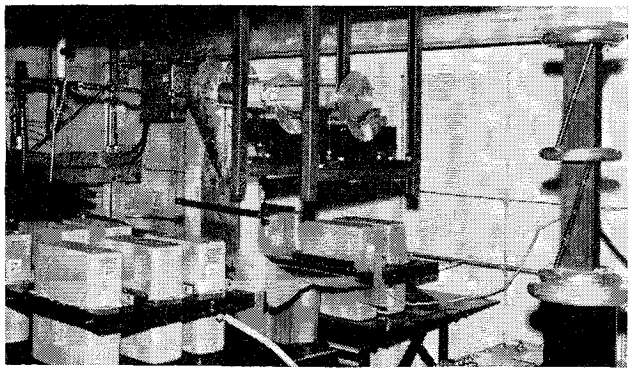

Fig. 1 Thermal impact facility

film of platinum to promote reflection of the short-wavelength waves. End caps enclose the second focus of the ellipsoids, at which samples may be placed.

One side of the cartridge provides a vacuum port and/or a focus for spectroscopic measurements. At the other side, specimens are irradiated directly or at the focal point of the mirror. The glass samples are $\frac{3}{4}$ in. in diameter and of any thickness. The pressure in the system is maintained at 10^{-4} mm-Hg. At this pressure, the mean free path is 50 cm, so that shock waves are not formed, and the density is low enough to prevent excessive attenuation of short waves.

III. Experimental Procedure

A. General Summary

Pyrex or lime glass disks were cleaned thoroughly and examined for flaws before exposure. They were placed in the cartridge or at the focus of the ellipsoidal mirrors. The damage that occurred on the exposed surface was measured with a stereo-microscope and a profilometer. The longest cracks were several millimeters long, and the shortest were less than 0.1 mm. Different samples exposed to different power levels showed cracks of various lengths and number.

B. Black Body Radiation Experiment

The effects of radiant energy transfer using the full equipment have been shown. The wires were exploded at one focal point of the ellipsoidal mirror and a pyrex or soft glass disk sample placed at the second focal point. The pressure was reduced to 10^{-4} mm-Hg to preclude the formation of a shock wave. A blinder was placed between the mirror halves to intercept direct radiation and direct particle travel. Therefore, all energy reaching the sample arrived only after reflection from the mirror wall.

The damage caused by the wire explosion is shown in Fig. 3. On the actual samples, the crack lengths varied from 0.1 to 3 mm, depending upon the power level of the explosion.

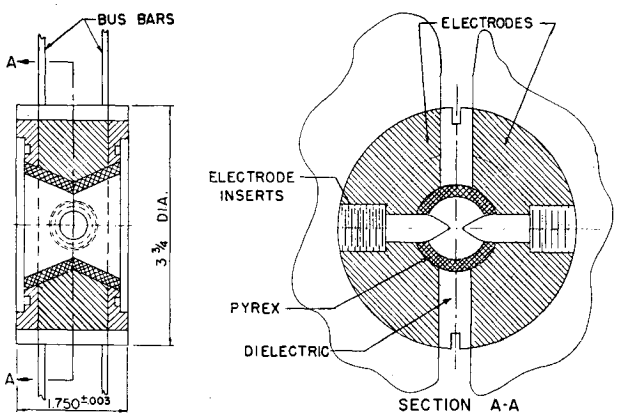

Fig. 2 Basic discharge cartridge

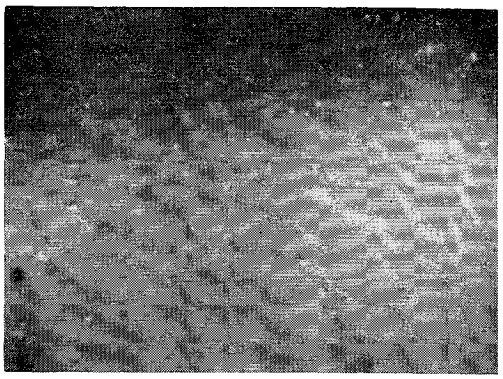

a) Energy stored = 400 joules

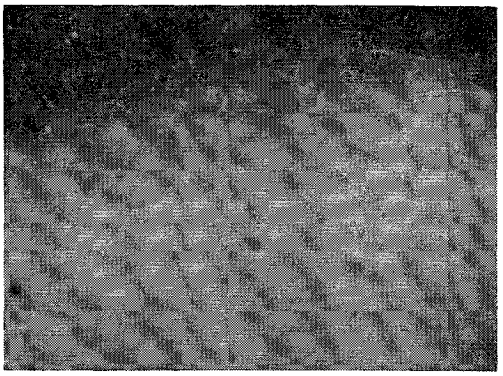

b) Energy stored = 600 joules

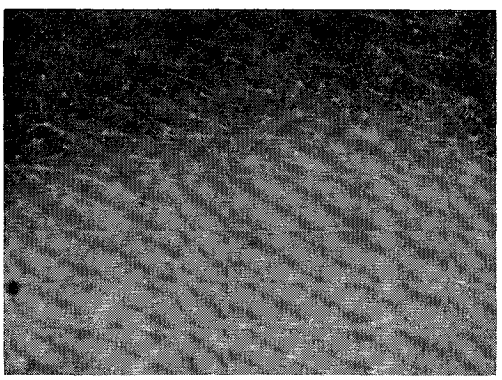

c) Energy stored = 900 joules

Fig. 3 Cracks in Pyrex (30×)

One notices that the density of cracks increases with the energy level.

Figure 4 shows another photomicrograph of damage caused by capacitor discharge from a higher energy level, in which the cracks are similar to those produced by a shattering blow. Long cracks sweep across the surface with interconnecting shorter cracks. Chips that form may be lifted out of the surface. After several chips were removed, a Brush Electronics Company profilometer was used to determine that the crack and chip depth is $\frac{1}{2}$ mil (about 10^{-3} cm). See Fig. 5.

C. Shock Wave Experiment

When open to the atmosphere, the equipment is capable of creating a shock wave that not only is heard several laboratories away but also is capable of shattering the cartridge chamber walls. With a glass disk at the cartridge ($\frac{3}{4}$ in. from the wire), the shock was large enough at 1000 joules stored (but not at 700 joules) to shatter the glass. Figure 6 shows the results. The plates were cracked at atmospheric pressure, at 1-mm-Hg pressure, and at 0.1 mm. However,

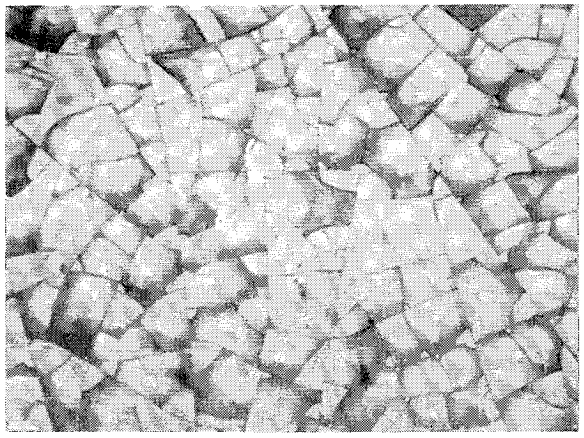

Fig. 4 Photomicrograph of bubbly surface (82×); sample at focus of ellipsoidal mirrors; energy stored = 3000 joules

at pressure lower than 10^{-3} mm, the plate showed no tendency to crack even at 3000 joules stored in the capacitor banks. Figure 7 shows the relation between pressure in a chamber and the dimensions of the chamber needed to form a shock wave. This distance is nominally ten times the mean free path of the gas molecules. At a pressure of 10^{-4} mm, the mean free path is 51 cm. Therefore, the shock wave is ruled out as a cause for the damage, such as seen in Fig. 4.

D. Convective Heat Transfer

Damage by plasma contact was illustrated by placing glass samples next to the exploding wire so that the plasma would envelop the sample when it explodes. The pressure was lowered to 10^{-5} mm to reduce attenuation of the plasma during its travel. Microscope slide covers 8-mil thick were supported on standoff pedestals at points $\frac{1}{4}$, $\frac{1}{2}$, and $\frac{5}{8}$ in. from the wire. Figure 8 shows photographs of the results. (The gross breaks were caused by nervous personnel.) When viewed by eye or with a stereo-microscope, long slivers stick up in graceful curves away from the surface. Their thickness is $\frac{1}{15}$ that of the slide, or $\frac{1}{2}$ mil (10^{-3} cm). This value agrees with that found previously for the black body radiation experiment.

Two patterns form: 1) the shavings peel either radially away from or toward the center support, and 2) the shavings follow a general horizontal direction on the plate. An explanation is proposed as follows. Assume that the surface is heated by absorbing energy when in contact with the surrounding plasma. The temperature distribution has a large gradient in the sample with the temperature varying by an order of magnitude. A preferential yielding occurs at the surface, so that the stresses fall to a low value. Upon cooling and contraction, the surface is subjected to tensile stresses, whereas the lower layers (not having yielded) retain compressive stresses. Cracks are formed in the tension field which propagate to the surface, thereby liberating one end of the chips. Part of the stress is relieved, but the moment cannot be relieved so readily. The remaining moment curls the chip out of the plane of the surface. There are also square chips left standing on edge which have not curled because of their two-directional flexural rigidity. This

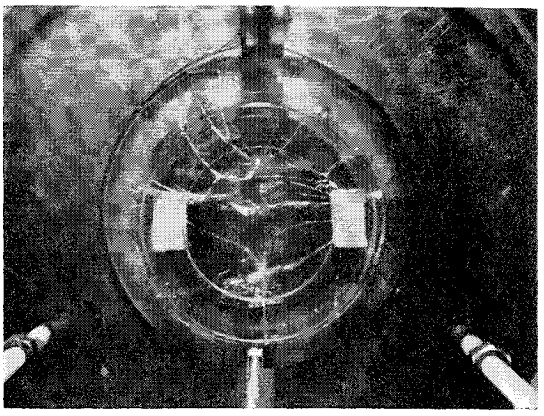

Fig. 6 Shattered glass on chamber

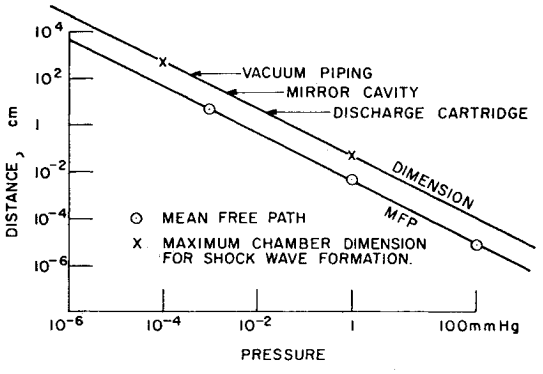

Fig. 7 Shockwave formation characteristics

type of damage occurred for all positions of the sample in the chamber. In fact, the rear of the sample was similarly damaged when the plasma could surround the plate completely.

E. Particle Impact

Particle damage is shown by pock marks on the glass surface. Figure 3 shows these to be uniformly dense over the entire surface. They occur quite independently of the cracks; that is, sometimes at an end of the crack, sometimes along the length of the crack, and many times between cracks. If a crack were formed by an impacting particle, one would expect to find "stars" at pock marks. Because stars do not occur, and because the pock marks are not related to the cracks, the two effects are believed to be produced independently.

IV. Theoretical Discussion

Damage in the glass surface has been postulated to be caused by thermally induced stresses. A derivation given in Appendix A starts with the energy stored in the capacitors and carries through to a prediction for the stress in the glass.

A. Black Body Radiation

For the black body radiation type of energy transfer, the divergence of the Poynting vector has been used as a heat

Fig. 5 Profilometer record of surface

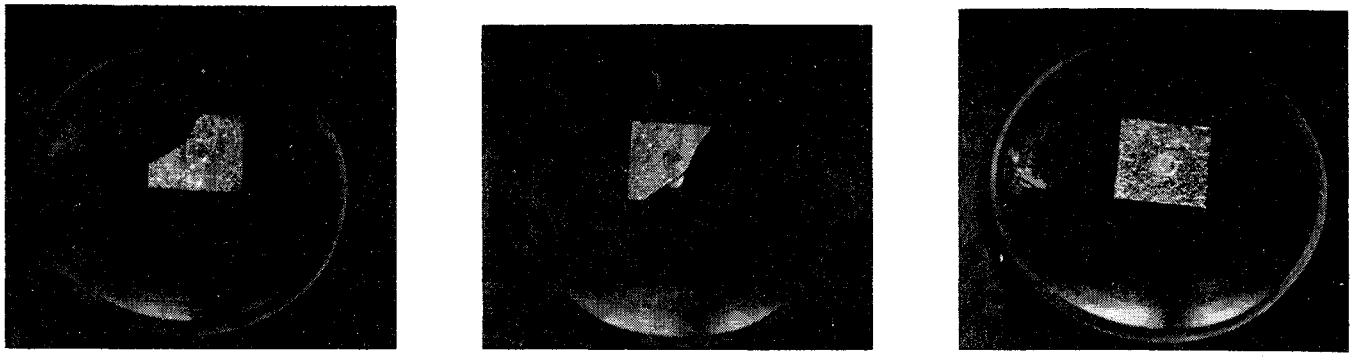

a) $\frac{1}{4}$ in. from wire b) $\frac{1}{2}$ in. from wire c) $\frac{5}{8}$ in. from wire

Fig. 8 Photograph of exposed microscope slide

source in the standard heat diffusion equation. Because this heat source is an exponential function, the exact solution of the differential equation for the temperature involves error functions and other exponentials. Figure 9 shows the temperature distribution. As explained in Appendix A, it is concluded from the position of the steep slope that the absorption coefficient must be of the order of 10^3 cm^{-1}.

The maximum ordinate for the curve with the absorption coefficient equal to 10^3 cm^{-1} is 1.6×10^{-2} deg cm^2 sec/cal, which is the ratio of the rise in temperature to the Poynting vector magnitude. Since neither is known, values are chosen which are reasonable for the equipment. For a temperature of 200°C, the energy deposited in a 10-μ sec pulse is $\frac{1}{2}$ joule/cm^2. For 400°C, the deposited energy would be 1 joule/cm^2.‡ These values are well within bounds for the equipment.

The electromagnetic waves are assumed to be plane, so that the temperature is a function of x alone. With this planar distribution, the stresses and strains in the glass also will be constant over planes parallel to the surface. The glass has been assumed to be a semi-infinite body, since the temperature at the rear face is not changed during the first 10 μsec, the duration of the pulse. The stress in the x direction must be zero because the stress at the surface is zero.[8] For the planar stress condition,

$$\sigma_y = \sigma_z = \sigma \tag{1}$$

$$\epsilon_y = \epsilon_z = 0 \tag{2}$$

because of the semi-infinite body stipulation. Hook's law then states that

$$0 = \alpha T + \sigma(1 - \nu)/E \tag{3}$$

and

$$\sigma(x, t) = \alpha T(x, t)E/(1 - \nu) \tag{4}$$

in which α is the coefficient of expansion of the glass, E is Young's modulus, and ν is Poisson's ratio.

The stress is related directly to the temperature by a constant. Thus, the approximations for the temperature distributions are valid for the stresses, also.

Glass is a brittle material that always fractures at stresses much less than one would expect from theoretical calculations. Griffith, in his crack theory advanced in 1921 and still accepted today,[9] calculated the fracture propagation stress by setting the strain energy released equal to the work required to form a new surface. Flaws that are present in glass at all times become stress raisers from which cracking starts when the glass is put under stress. After studying the relationships between flaw geometry and stress concentration, Griffith proposed the following expression for the critical stress needed to propagate a crack:

$$\sigma_{cr} = (4ES/\pi w)^{1/2} \tag{5}$$

where S is the surface energy, E is Young's modulus, and w is the crack width.

Even though the thermal stresses are compressive, at the ends of elliptical voids there will be tensile stresses to which Griffith's criterion might be applied. On the other hand, the same criterion could be applied to compressive stresses if a correction factor may be included in calculating the critical stress. (Orowan[10] and others[11, 12] state that the factor should be between 3 and 8.) In that event, the glass may crack when it is heated. On the other hand, the glass may yield when hot, so that, upon cooling, tensile stresses will develop which can exceed the critical stress (without the correction factor) and crack the glass.

A temperature of 200°C produces a stress of 27,000 psi in glass. This is greater than the tensile strength of glass (5000 psi).[13] In compression, this stress probably would not crack the glass unless residual strains were present further to increase the effective stress. By the same token, if the strains were relieved by yielding an amount equivalent to a temperature drop of 100°C, the tensile stress produced by cooling 150° would be 7000 psi, which will crack the glass in tension. These rough calculations show that the glass will crack during the test. Whether these cracks and chips form in compression or in tension must be determined experimentally. Tests are now in progress to measure the time of cracking.

B. Convective Heat Transfer

When the plasma contacts the sample, heat is transferred as each ion or particle meets the sample. This process is similar to that of "contact with a well-stirred fluid." The solution to the heat diffusion equation is given by Carslaw and Jaeger,[14] for this instance. The solution again is given in terms of the error function, and the temperature distribution is similar to that shown in Fig. 9. Therefore, similar results would be expected with the effects of a higher surface temperature accentuated.

V. Conclusion

In conclusion, we note that four methods have been postulated for transferring energy from the wire to the glass surface at which damage occurred. 1) Radiant energy was shown to be powerful enough to crack the glass surface. Theoretical derivations were advanced to support this claim using the

‡ Values for this temperature are not quoted in the literature, because measurements have so wide a spread that one can obtain only probable values. Therefore, this temperature range has been chosen as an order-of-magnitude value.

thermal diffusion and thermal elastic equations and Griffith's incipient flaw theory. 2) Shocks were found to be strong enough to shatter the chamber walls, but not when the pressure in the chamber was reduced to 10^{-4} mm Hg. 3) Convective heat was shown to be sufficient to crack the surface if the sample were close enough to the exploding wire, about 1 in. By moving the sample to a position 28 in. away (to the second focal point of thee llipsoidal mirror), plasma contact was prevented. 4) Particle kinetic energy was indicated as occurring even at the far point. However, both at this point and at near points, the effect of the impinging particles was shown to be independent of the other effects.

Cracks thus occur on glass surfaces exposed to an exploding wire in a vacuum for two conditions. When the glass is far away from the wire, an intense radiation pulse will heat the glass with a transient that will crack the surface. When it is close to the wire, the plasma that contacts the glass heats the surface to a temperature at which the thermal stresses are relieved. Upon subsequent cooling, the tensile stresses crack the glass and curl chips up and out of the surface.

Appendix: Derivation of Temperature Distribution in the Sample

The absorption of electromagnetic radiations depends upon the electrical conductivity of the medium. For our glass samples, the absorptivity varies from 10^{-3} to 10^{6} cm^{-1}, depending upon the wavelength of the radiation. Any damage caused by the exploding wire will occur because of an integral effect of all waves striking the sample. Thus, an average absorption constant will be determined from the results, since no dispersive device was used. From Poynting's vector S, one finds that the energy deposited ($\nabla \cdot S$) by a wave passing through a medium depends directly on the absorption constant b and exponentially on the negative product of the absorption constant and the distance into the medium x.[15] Thus,

$$\nabla \cdot S = Pbe^{-bx}$$

where P is the proportionality constant.§

Given this energy dissipation, the distribution of temperature may be found by solving the thermal diffusion equation

$$K(\partial^2 T/\partial x^2) - c\rho(\partial T/\partial t) + Pbe^{-bx} = 0$$

for the temperature T as a function of x the distance and t the time. K,c, and ρ are the thermal conductivity, specific heat, and density of the sample. These are assumed to be independent of x,t, and T. With the boundary condition that heat is reradiated at the front surface and the sample is a semi-infinite body initially at ambient temperature, the solution for T is given as

$$T(x,t) = \frac{P}{K}\left\{\frac{H+bK}{bH}\left[1 - \operatorname{erf}\frac{x}{2(Kt/c\rho)^{1/2}}\right] + \frac{1}{2b}\exp\left(\frac{-bx + Kb^2t}{c\rho}\right)\left[1 + \operatorname{erf}\frac{x - 2Kbt/c\rho}{2(Kt/c\rho)^{1/2}}\right] - \left[\frac{H+Kb}{2b(H-Kb)}\right]\exp\left(\frac{bx + Kb^2t}{c\rho}\right)\left[1 - \operatorname{erf}\frac{x + 2Kbt/c\rho}{2(Kt/c\rho)^{1/2}}\right] + \left[\frac{K^2b}{H(H-bK)}\right]\exp\left(\frac{Hx/K + H^2t}{Kc\rho}\right)\times\left[1 - \operatorname{erf}\frac{x + 2Ht/c\rho}{2(Kt/c\rho)^{1/2}}\right] - \left(\frac{1}{b}\right)\exp(-bx)\right\}$$

§ It is true that P will be a function of time as well as of the permittivity and conductivity. It is probably of the form $P = P_0 t^n e^{-qt}$, where n may be 0, 1, 2, or 3, and q is another positive constant depending upon pulse shape. By using a square pulse, n and q become zero within the pulse, and P_0 becomes zero outside the pulse. From photoelectric cell measurements, a square pulse is adequate to describe the pulse.

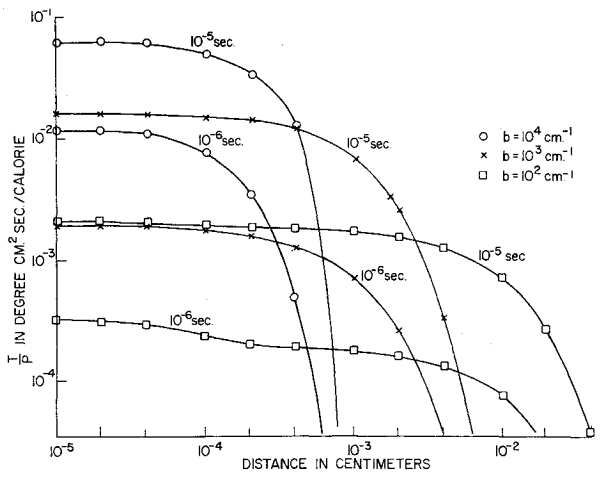

Fig. 9 Computed temperature profiles for various values of the absorptivity parameter b

where erf$z$ is the error function and H is the heat transfer coefficient.

The temperatures so obtained are shown on Fig. 9. The temperature divided by the constant irradiating flux P is plotted against the distance below the surface. The curves are plotted in pairs for three values of the absorption coefficient b. The lower curve of each pair represents the temperature after 1 μsec, and the upper curve represents the value after 10 μsec, the end of the pulse.

From the curves note these items: 1) as the absorption coefficient increases, the temperature increases; 2) as the absorption coefficient is increased by an order of magnitude, the quantity of material heated to near maximum drops by nearly an order of magnitude during the pulse of 10 μsec; 3) the temperature increases by an order of magnitude during the 10-μsec pulse; and 4) since thermal stresses are expected at temperatures in the hundreds of degrees centigrade, the important portions of the curves are within one order of magnitude of their maximum. By noting these items and by comparing Fig. 9 with the experimental data, the values of the absorption coefficient and the incident flux may be estimated.

The cracks and chips in the glass extended to a depth of 10^{-3} cm, as shown on Fig. 5 from profilometer data. Looking at the $b = 10^4$ cm^{-1} curves, one finds that the temperature starts to drop quite rapidly at a distance of 10^{-4} cm. Thus, if b had this value (10^4 cm^{-1}), the cracks must have propagated into the glass ten times as far as the distance to the surface in order to produce the chips. This feat is considered unlikely. Looking at the $b = 100$ cm^{-1} curves, one finds that the temperature would have been substantially the same after 10 μsec to a depth of 4×10^{-2} cm. In this case, one would expect that the glass should have cracks to at least 10^{-2} cm. This was not case-proven in the experiment. On the other hand, looking at the $b = 1000$ cm^{-1} curves, one sees that the temperature holds up almost to 10^{-3} cm and then drops rapidly. According to the foregoing reasoning, one would say that the absorption coefficient must be of the order of 10^3 cm^{-1}.[16]

References

[1] David, E., "Physikalische Vorgänge bei elektrischen Drahtexplosionen," Z. Phys. **150**, 162–177 (1958).

[2] Conn, W. M., "The use of exploding wires as a light source of very high intensity and short duration," J. Opt. Soc. Am. **41**, 445–449 (1951).

[3] Vanyukov, M. P. and Mak, A. A., "High intensity pulsed light sources," Sov. Phys.—Usp. **66**, 137–155 (1958).

[4] Lebedev, S. V., "Explosion of a metal by an electric current," Sov. Phys. JETP **5**, 243–255 (1957).

[5] Bennett, F. D., "Flow fields produced by exploding wires,"

Exploding Wires, edited by W. G. Chace (Plenum Press Inc., New York, 1952), pp. 211–226.

[6] Dugdale, R. A., Maskrey, J. T., and McVickers, R. C., "Some effects of thermal shock produced by intense gas discharges," Brit. Cer. Soc. Trans. **60**, 427–448 (1961).

[7] Anderson, J. A. and Smith, S., "General characteristics of electrically exploded wires," Astrophys. J. **64**, 295–314 (1926).

[8] Timoshenko, S. and Goodier, J. N., *Theory of Elasticity* (McGraw-Hill Book Co. Inc., New York), 2nd ed., p. 201.

[9] Griffith, A. A., "The phenomena of rupture and flow in solids," Phil. Trans. Roy. Soc. London A **221**, 163–198 (1951).

[10] Orowan, E., "The mechanism of seismic faulting," Symposium on Rock Deformation, Inst. Geophys., Univ. Calif., Los Angeles, Calif. (November 1956).

[11] Charles, R. J., "A review of glass strength," General Electric Res. Lab. Rept. 60RL-2314M (January 1960).

[12] Anderson, O. L., "The Griffith criterion for glass fracture," *Fracture*, edited by B. L. Averbach (John Wiley and Sons, Technology Press Mass. Inst. Tech., Cambridge, Mass., 1959), Chap. 17.

[13] Kee, H., "High temperature properties of glass," Prod. Eng. **32**, 84–87 (October 16, 1961).

[14] Carslaw, H. S. and Jaeger, J. C., *Conduction of Heat in Solids* (Clarendon Press, Oxford, 1959), p. 350.

[15] Stratton, J. A., *Electromagnetic Theory* (McGraw-Hill Book Co. Inc., New York, 1941), p. 281.

[16] Good, R. C. "Effects of electromagnetic waves radiated by an exploding wire," Bull. Am. Phys. Soc. **7**, 501 (1962).

JUNE 1963 AIAA JOURNAL VOL. 1, NO. 6

Thermal Properties of a Simulated Lunar Material in Air and in Vacuum

E. C. Bernett,* H. L. Wood,† L. D. Jaffe,‡ and H. E. Martens§
Jet Propulsion Laboratory, California Institute of Technology, Pasadena, Calif.

The thermal diffusivity and thermal conductivity for a crushed olivine basalt were determined from transient state data. Values were obtained over a temperature range of −100° to 200°C in vacuums of 5×10^{-3} and 5×10^{-6} mm Hg as well as at atmospheric pressure. A −150 mesh material at a density of 1.14 g/cm³ had a thermal conductivity of 3.9×10^{-6} cal/cm-sec-°C at 100°C when measured in a vacuum of 5×10^{-6} mm Hg. This was approximately 100 times lower than the values obtained for the same material measured at atmospheric pressure. Increasing the density to 1.57 g/cm³ increased the thermal conductivity by approximately 60% in both air and vacuum. Over the range studied, the test temperature had very little effect on thermal conductivity in air but showed more of an effect when the material was placed in a vacuum.

I. Introduction

In preparation for manned landings on the moon, research aimed at determining the physical and mechanical properties of the postulated lunar surface is now in progress. There have been extensive astronomical studies of the moon and its surface; on the basis of these, it is proposed that the moon is composed of igneous rocks similar to certain types that are found on earth. Some measurements,[1–3] however, indicate that the thermal conductivity of the lunar surface is extremely low—much lower than that of any known types of consolidated rock. To account for this, it is postulated that large portions of the lunar surface are covered with a highly porous material, probably powdery and perhaps lightly sintered.

The investigation described here is one part of a program designed to evaluate the properties of a powdered rock simulating the postulated lunar surface material. Its purpose was to measure the effects of vacuum on the thermal diffusivity and conductivity of rock powder.

Received by IAS November 26, 1962; revision received March 25, 1963. This paper presents the results of one phase of research carried out at the Jet Propulsion Laboratory, California Institute of Technology, under Contract No. NAS 7-100, sponsored by NASA.

* Research Group Supervisor.
† Test Engineer.
‡ Chief, Materials Research Section. Member AIAA.
§ Assistant Chief, Materials Research Section.

II. Materials Tested

The material used in the initial runs, which were designed to check equipment operation, was a 70-mesh commercial grade 99% silica foundry sand. The particle size distribution of this material is shown in Fig. 1. The moisture content was less than 0.03%.

The material selected to simulate lunar material for this study was an olivine basalt collected from Pisgah Crater, San Bernardino County, Calif. The large volcanic bombs were crushed to about 3-in. size using a hydraulic press. Any pieces that appeared to be contaminated or that showed signs of weathering were discarded. The remaining material was passed through a Gates jaw crusher and a stainless-steel hammer mill-type pulverizer to reduce it all to −35 mesh material. A detailed mineralogical description of this material and the crushing procedure is given in Ref. 4.

Most of the −35 mesh material was screened into more closely sized fractions: nominally −35 +48, −48 +65, −65 +100, −100 +150, and −150 mesh. Actual screen analyses of the fractions used for the thermal conductivity tests are shown in Fig. 1.

The "as-received" density of the rock as measured by water displacement was 2.83 g/cm³ at 24°C. The density of the crushed material was 2.97 g/cm³. All of the screened fractions were stored in closed containers. Measurements made during the program showed that actual moisture content varied from day to day but always was less than 0.1%.